OXFORD

SOT | Society of Toxicology
www.toxsci.oxfordjournals.org

TOXICOLOGICAL SCIENCES, 156(2), 2017, 492–508

doi: 10.1093/toxsci/kfx010
Advance Access Publication Date: January 13, 2017
Research article

Neuropathological Consequences of Gestational Exposure to Concentrated Ambient Fine and Ultrafine Particles in the Mouse

Carolyn Klocke,*[,1] Joshua L. Allen,* Marissa Sobolewski,* Margot Mayer-Pröschel,† Jason L. Blum,‡ Dana Lauterstein,‡ Judith T. Zelikoff,‡ and Deborah A. Cory-Slechta*

*Department of Environmental Medicine; †Department of Biomedical Genetics, University of Rochester School of Medicine, Rochester, New York 14642; and ‡Department of Environmental Medicine, New York University School of Medicine, Tuxedo, New York 10987

[1]To whom correspondence should be addressed. E-mail: carolyn_klocke@urmc.rochester.edu.

ABSTRACT

Increasing evidence indicates that the central nervous system (CNS) is a target of air pollution. We previously reported that postnatal exposure of mice to concentrated ambient ultrafine particles (UFP; ≤100 nm) via the University of Rochester HUCAPS system during a critical developmental window of CNS development, equivalent to human 3rd trimester, produced male-predominant neuropathological and behavioral characteristics common to multiple neurodevelopmental disorders, including autism spectrum disorder (ASD), in humans. The current study sought to determine whether vulnerability to fine (≤2.5 μm) and UFP air pollution exposure extends to embryonic periods of brain development in mice, equivalent to human 1st and 2nd trimesters. Pregnant mice were exposed 6 h/day from gestational days (GDs) 0.5–16.5 using the New York University VACES system to concentrated ambient fine/ultrafine particles at an average concentration of 92.69 μg/m^3 over the course of the exposure period. At postnatal days (PNDs) 11–15, neuropathological consequences were characterized. Gestational air pollution exposures produced ventriculomegaly, increased corpus callosum (CC) area and reduced hippocampal area in both sexes. Both sexes demonstrated CC hypermyelination and increased microglial activation and reduced total CC microglia number. Analyses of iron deposition as a critical component of myelination revealed increased iron deposition in the CC of exposed female offspring, but not in males. These findings demonstrate that vulnerability of the brain to air pollution extends to gestation and produces features of several neurodevelopmental disorders in both sexes. Further, they highlight the importance of the commonalities of components of particulate matter exposures as a source of neurotoxicity and common CNS alterations.

Key words: neurotoxicology; air pollution; white matter; myelin.

Air pollution is a global environmental health concern (Lelieveld *et al.*, 2015) associated with respiratory and cardiovascular disease morbidity that is considered to occur via inflammatory mechanisms (Kelly and Fussell, 2015). While the magnitude and range of its toxic effects are highly dependent upon composition and concentration of constituent pollutants (Bell *et al.*, 2009), evidence shows that the particulate matter (PM) fraction of air pollution is a major contributor to adverse health effects. PM toxicity is highly dependent on particle size, with coarse particles (≥10 μm, PM_{10}), considered to be the least toxic as they are generally trapped and cleared within the upper airway (Sturm, 2013), and fine particles (≤2.5 μm, $PM_{2.5}$) currently regulated by the U.S. Environmental Protection Agency (US EPA). Evidence suggests that both fine and coarse PM

exposures are associated with increased cardiovascular and respiratory morbidity and mortality (Adar *et al.*, 2014), as well as a wide spectrum of neuropathologies (Block and Calderón-Garcidueñas, 2009). Ultrafine particles (UFP; ≤100 nm, $PM_{0.1}$), considered the most reactive because of their small size (Oberdörster, 2000), penetrate deeper into lung (Terzano *et al.*, 2010) and have a higher surface-to-volume ratio that increases the potential for cellular adsorption (Oberdörster *et al.*, 2004). The small size and physical characteristics of UFP increase the potential for adsorption of additional toxicants onto the particle itself (Penn *et al.*, 2005), including heavy metals, bacterial lipopolysaccharide (LPS), and polyaromatic hydrocarbons (PAHs). Because of these characteristics, UFPs are putatively the most toxic air pollution component, yet there are currently no US EPA regulations regarding exposure to these particles.

Increasing evidence suggests that the central nervous system (CNS) is both a direct and indirect target of air pollution, chiefly the fine and UFP components. Direct CNS localization of UFP can occur after intranasal instillation via translocation across the olfactory epithelium and olfactory nerves (Oberdorster *et al.*, 2004, 2009). Indirectly, it has been demonstrated that UFP can translocate to the brain after tracheobronchial instillation via transport along sensory afferent nerves. These routes of particle translocation are known to elicit a neuroinflammatory response (Block and Calderón-Garcidueñas, 2009). Additionally, PM may indirectly affect the CNS by inducing peripheral release of soluble proinflammatory mediators (Fujii *et al.*, 2001; Mumaw *et al.*, 2016). PM deposited in lung is also capable of inducing a neuroinflammatory response by stimulation of the vagal nerve (McQueen *et al.*, 2007). Overall, these observations demonstrate that the particulate fraction of air pollution acts as an inflammatory stimulus and is capable of inducing neurotoxicity through multiple direct and indirect mechanisms.

The brain is particularly sensitive to environmental insults during development, and given the multiple mechanisms by which particulates and other pollutants can impact brain, gestation is a period of particular concern for air pollution exposure. Given the precisely timed nature and ongoing synchronization of cell division, migration and maturation, the gestational period presents numerous critical windows during which an environmental insult could disrupt the normal course of neurodevelopment. These critical windows of neurodevelopment have been increasingly implicated in the increased number of reported associations of air pollution with neurodevelopmental disorders, including autism spectrum disorders (ASD) and schizophrenia, as well as with cognitive and attention deficit syndromes (Kalkbrenner *et al.*, 2015; Siddique *et al.*, 2011; Yackerson *et al.*, 2013). Increased risk for ASD and schizophrenia and associated neuropathology has also been described in the context of maternal infection and systemic inflammation during pregnancy (Meyer *et al.*, 2011). As air pollution is a known inducer of systemic inflammation in humans (Kelly and Fussell, 2015), it is possible that a pollutant-induced inflammatory response in a pregnant female increases the risk of neuropathology in the offspring.

Previous studies from our laboratory in mice provide biological plausibility for a role of developmental air pollution exposure in neurodevelopmental disorders. Exposure to concentrated ambient UFP during the early postnatal period, a time of rapid neuro- and gliogenesis (Bandeira *et al.*, 2009) and considered equivalent to human 3rd trimester (Rice and Barone, 2000), produced persistent and male predominant inflammation/microglial activation (Allen *et al.*, 2014a; Allen *et al.*, 2014c), reductions in corpus callosum (CC) size with associated hypomyelination and ventriculomegaly (Allen *et al.*, 2014a, 2015), elevated glutamate and excitatory/inhibitory imbalance (Allen et al., 2014a, 2014b), increased amygdala astrocytic activation (Allen *et al.*, 2014a), and repetitive and impulsive behaviors (Allen *et al.*, 2013). Given the possibility from these earlier studies that air pollution could serve as a broad risk factor for neurodevelopmental disorders, we hypothesized that this vulnerability extends to even earlier periods of brain development and, additionally, we sought to determine if gestational exposure produces sexually dimorphic effects, e.g. a male-predominant pathology such as that observed previously in postnatal-only exposures.

The gestational period encompasses a significant time of brain development during which essential micronutrients, such as metals, are acquired by the fetus via placental transfer in the pregnant female. Given that metal homeostasis is tightly regulated during fetal development (Kambe *et al.*, 2008), perturbations of metal levels can alter the trajectory of neurodevelopmental endpoints and induce pathology. Notably, extensive studies of iron in relation to neural development demonstrate that alterations in iron levels, i.e. iron deficiency, disrupts CNS development and produces characteristic neurological sequelae, including protracted cognitive impairment and reductions in brain myelin (Radlowski and Johnson, 2013). Dysregulation of metal homeostasis may play a key role in air pollution mediated neurotoxicity, as metals are often a key component in PM (Block and Calderón-Garcidueñas, 2009). Air pollution exposures completed using the experimental methods described here are known to contain elevated levels of elemental metal species when compared to controls (Blum *et al.*, 2013), and, of these, iron has been extensively characterized as a regulator of brain fatty acid biosynthesis and myelin formation in models of iron deficiency (Todorich *et al.*, 2009). Elevation of fetal iron levels could likewise be detrimental to CNS development, as iron overload is a known inducer of oxidative stress and has demonstrated neurotoxicity *in vitro* and in adult mouse models (Bresgen and Eckl, 2015). Currently, information regarding the effects of iron overload on neurodevelopment is lacking. This study additionally sought to determine whether elevated iron levels in concentrated ambient exposures disrupt brain iron levels and correlate with any observed neuropathology in mice exposed gestationally to fine and UFPs.

MATERIALS AND METHODS

Animals and Air Pollution Exposures

Male and female 8–10-week-old B6C3F1 hybrid mice (Jackson Laboratory, Bar Harbor, ME) were paired. Upon discovery of a coital plug (GD0.5), females were removed, weighed, assigned to a treatment group and placed into the exposure box. Timed-pregnant dams ($N = 16$) were exposed to concentrated ambient fine and ultrafine particles (CAPs) or HEPA-filtered air (FA) via compartmentalized whole-body inhalation for 6 h/day from GD0.5 through GD16.5 using the Versatile Aerosol Concentration Enrichment System [VACES; New York University Department of Environmental Medicine, Sterling Forest, New York; (Maciejczyk *et al.*, 2005)]. This system was chosen to test whether spatiotemporal variability in air pollution composition would produce similar neuropathological effects as previously observed, i.e. ventriculomegaly and glial activation. The VACES system concentrates PM at a comparable factor when compared to the Rochester HUCAPS system used in previous studies (Allen *et al.*, 2013; Allen *et al.*, 2014a; Allen *et al.*, 2014b; Allen *et al.*, 2014c; Allen *et al.*, 2015).

The particle size distribution of the VACES system is slightly larger than the HUCAPS but still within the fine/ultrafine range (Kim *et al.*, 2001). Exposures occurred between 08:00 and 14:00 hours during August of 2014. Dams had access to food and water *ad libitum* except during exposures and were weighed daily to assess any effects of exposure on gestational weight gain. Beyond the final day of exposure (GD16.5), dams were maintained in ambient air through birth and the postnatal period. The timepoint of PND 11–15 for assessment of brain outcomes was selected as this period encompasses the peak of myelination, and given the magnitude of myelin biosynthesis that occurs during this time, PND was controlled for statistically (described in **Statistical Analyses**). No offspring mortality was observed and sex of the offspring was determined by visual examination. Final offspring sample numbers were: 11 female FA, 7 female CAPs, 9 male FA, and 6 male CAPs from 5 to 6 litters/treatment group. Mice used in this study were treated humanely and all study protocols were approved by the New York University Institutional Animal Care and Use Committee.

Elemental Characterization and Mass Concentration of Collected Particles

Mass concentration of CAPs exposures was determined daily using pre-weighed Teflon filters (37 mm, 0.2 μm pore size; Pall, Port Washington, New York). Particle-laden filters were equilibrated overnight in a temperature/humidity controlled room (21 °C ± 0.5 °C and 40 ± 5% relative humidity) and weighed gravimetrically on a MT5 microbalance (Mettler Toledo, Hightstown, New Jersey). X-ray fluorescence spectroscopy (XRF) was used to determine the elemental composition of exposures. Briefly, filters from every third exposure day were analyzed using an ARL QUANT'X EDXRF Analyzer (ThermoFisher Scientific, Waltham, Massachusetts). Lot-matched, unexposed filters were used as blank controls.

Tissue Preparation, Histological Staining, and Image Analysis

Pups were sacrificed by rapid decapitation between PND 11-15, and brains extracted, hemisected, and fixed in 4% paraformaldehyde for 24 hours and postfixed in 30% sucrose until they completely sank. Tissue from the left hemisphere was sectioned in the sagittal plane at 40 μm into cryoprotectant (30% sucrose and 30% ethylene glycol in 1.0M phosphate buffer) and stored at −4 °C until immunostaining. Every 6th section was stained for ionized calcium binding adapter molecule 1 (Iba-1, 1:5000; Wako, Richmond, Virginia) or myelin basic protein (MBP, 1:1000; Millipore, Billerica, Massachusetts) to assess microglial activation and myelination status, respectively, as previously described (Allen *et al.*, 2014a, 2014b, 2014c, 2015). MBP and Iba-1 antibodies were reacted chromogenically using metal-enhanced 3,3′-diaminobenzidinetetrahydrochloride (DAB; Sigma Aldrich, St. Louis, Missouri). FluoroMyelin Red staining was carried out according to manufacturer's instructions (ThermoFisher Scientific, Walktham, Massachusetts) to determine the presence of compact myelin in the CC. Slide-mounted tissue sections were visualized on an Olympus BX41 microscope (Olympus America, Inc., Central Valley, Pennsylvania) mounted with an MBF CX9000 camera (MBF, Villiston, Vermont) for myelination image capture.

All analyses were performed by a single experimenter blinded to treatment conditions. To quantify myelin staining density, images were captured at 20X, merged using Photoshop Elements 11.0 (Adobe, San Jose, California), and analyzed using established thresholding methods (Cherry *et al.*, 2014) in ImageJ (National Institutes of Health, Bethesda, Maryland) to generate a percent area positive for staining. Unbiased stereology and anatomical area tracings were performed using Stereo Investigator or Neurolucida software (MBF, Williston, Vermont), respectively, with an Olympus BX53 microscope mounted with a Qimaging Retiga 2000R camera at 40× magnification, as previously described (Allen *et al.*, 2015). For stereological interrogation, the optical fractionator probe was used to sample at least 10% of each region across 3 tissue sections. The mean thickness of each sample was determined in 3 fields across all 3 tissue sections, and the upper and lower 0.5 μm limits were excluded from analysis. The microglial numbers per region are reported as actual counts and not software estimates of total region density.

Anatomical area tracings were sampled across 3–5 sections for each region of interest. A murine anatomical brain atlas (Franklin and Paxinos, 2007) was utilized in conjunction with identification of anatomical landmarks to ensure that sections of homologous bregma were analyzed between samples. However, it should be noted that this atlas typically serves as a reference for the adult mouse brain, and given the ongoing brain development at our selected timepoint, there may be slight variability in the regional specificity of the analyzed tissue sections. Given this, the approximate adult-equivalent bregma analyzed per endpoint ranged from 0.12 to 1.68 mm.

For brain region area measurements, averaged data are presented linearly from lateral to medial sections, i.e. averages from the lateral-most tissue section moving across the brain to averages from the medial-most sections. Myelin density is presented similarly, but in a rostral-to-caudal direction. In the case of frontal cortex thickness, data are presented linearly in 2 directions: lateral to medial and rostral to caudal. This was done as different areas of the large span of the frontal cortex might exhibit regional specificity in cortical thickness.

To determine whether the observed changes in hippocampal and CC areas and CC myelination were correlated with a neuroinflammatory phenotype, the level of microglial activation in both regions was scored where 1 = quiescent microglia with small cell bodies and fully ramified processes, 4 = activated microglia with amoeboid morphology and, at most, 2 partially ramified processes. Intermediate activation states were also identified, where 2 = partially ramified morphology with a larger (yet not fully amoeboid) cell body and similar ramification patterns compared to a fully ramified microglia, and 3 = mostly activated microglia with an amoeboid cell body that presents 3 or more processes. These activation states were modified from established methods (Hutson *et al.*, 2011). Microglial activation data are reported as averages across 3 tissue sections.

Iron levels in the CC were determined histologically using every 6th tissue section. Tissue was mounted onto gelatin subbed slides and then stained chromogenically using Perl's Prussian Blue stain for iron. Briefly, slides were hydrated to 100% ethanol prior to immersion in 5% potassium ferrocyanide (#3114-01, J.T. Baker, Central Valley, Pennsylvania) for 5 min. Slides were then submerged in a solution of 10% potassium ferrocyanide and 20% hydrochloric acid for 30 minutes, washed thoroughly in deionized water, and immersed in a filtered counterstain solution of neutral red for 3 min. After rinsing in deionized water, the stain was differentiated in 70 and 95% acetate buffered ethanol. Slides were then dehydrated and cleared using Histoclear (National Diagnostics, Atlanta, Georgia) and allowed to dry prior to coverslipping (Permount, #SP15-500,

Fisher Scientific, Waltham, Massachusetts). The total number of positively-stained iron inclusions was quantified in the entirety of the CC across 3 homologous tissue sections per brain. Histological iron data are presented as the average of the total number of inclusions across 3 tissue sections.

Statistical Analyses

Statistical analyses were conducted using JMP Pro 12.0 (SAS Institute Inc., Cary, North Carolina). Lateral ventricle, hippocampal and CC area were analyzed separately using a repeated measures ANOVA with treatment group (CAPs or FA), sex, and PND as fully factorial, between-group factors and tissue section as a continuous, within-group factor. PND was included as a factor as brains were collected between PNDs 11–15, a known period of significant brain development. Numbers and activation state of microglia as well as CC iron levels were analyzed separately by sex using one-way ANOVAs. Post hoc testing was conducted contingent on ANOVA outcomes using Student's *t*-test. Correlations between iron levels and CC area, myelin density, and microglial number were analyzed using linear regression. Statistically significant outliers were determined via Grubbs test and p values ≤ 0.05 were considered statistically significant.

RESULTS

Exposure and Litter Parameters

The mean CAPs concentration over the exposure period averaged 92.69 ± 19.16 (mean ± SD) μg/m^3 compared to 3.52 ± 0.87μg/m^3 for FA controls (Figure 1) as determined by weighing particles on pre-weighed Teflon filters. CAPs exposure levels ranged from 32.95 to 184.43μg/m^3 over the duration of the exposure period. CAPs exposure was not overtly toxic to dams and did not significantly affect maternal weight gain or reproductive success endpoints (Figure 1), litter size (mean ± SEM = 7.89 ± 1.96 for FA control and 8.42 ± 0.53 for CAPs), birth weights (1419.70 ± 41.71 mg for CAPs, 1396.91 ± 62.72 mg for FA) or crown-rump length at birth (CRL; 25.04 ± 0.40 mm CAPs, 25.09 ± 0.30 mm FA).

Brain Structure and Size

Both male and female CAPs-exposed offspring exhibited significant enlargement of the lateral ventricles compared to FA-exposed offspring (Figure 2), as confirmed by a main effect of CAPs treatment [$F(1,22) = 0.343$, $P = 0.012$]. Increases were seen across sections from lateral to medial CC. A PND by sex interaction was also found in the statistical analyses, which indicated differences by sex in ventricle growth across PND 11–15 [$F(1,22) = 0.197$, $P = 0.049$], with greater increases in area in males.

Analyses of the extent to which CAPs-induced ventriculomegaly was associated with changes in size of periventricular brain structures revealed (Figure 3a) a small but significant CAPs-induced reduction in hippocampal size across sexes [$F(1,26) = 10.658$, $P = 0.004$], with a significant sex-independent effect of PND [$F(1,16) = 10.618$, $P = 0.003$]; the latter reflects the changes in these markers by postnatal day, as expected. Surprisingly, gestational CAPs exposure increased the area of the CC (Figure 3b), the largest white matter tract in the brain, across sexes: (main effect of CAPs [$F(1,25) = 9.472$, $P = 0.005$], again with a sex-independent significant effect of PND [$F(1,25) = 40.329$, $P < 0.0001$]). Changes in cortical thickness are characteristic of neurodevelopmental disorders such as ASD and schizophrenia (de Lacy and King, 2013). Thus, frontal cortex thickness was measured in 2 directions through the brain, lateral-to-medial and rostral-to-caudal, in order to capture any discrete regional alterations in cortical thickness. Analyses of these endpoints revealed CAPs did not induce statistically significant changes in cortical thickness in either sex (Figure 4).

Myelination

Analyses of myelin basic protein expression level in CC revealed gestational CAPs exposures resulted in a higher staining density, suggestive of increased myelin production or a higher number of mature oligodendrocytes in both sexes when analyzed collapsed across the 3 major regions of CC, i.e., the splenium, the midbody, and the genu [$F(1,25) = 4.199$, $P = 0.0511$; Figure 5]. There was, as expected, a significant sex-dependent effect of PND on MBP expression [PND $F(1,25) = 38.197$, $P < 0.001$]; PND by sex [$F(1,25) = 4.904$, $P = 0.0361$] as PND11–15 represents a period of major brain myelination. There was also a suggestion (treatment*sex, $F(1,25) = 2.9145$, $P = .1002$) of an altered myelination pattern across CC in females that was not seen in males, specifically a greater myelin basic protein level expression in genu rather than midbody of females, but not males. To corroborate the findings of increased MBP expression, a protein component of myelin, tissue was stained with FluoroMyelin Red to detect the presence of compact myelin. Densitometric analysis revealed a significant increase in fluorescent staining density in both sexes as a result of CAPs exposure [$F(1,25) = 34.949$, $P < .001$; Figure 6]. As with MBP, there was a significant effect of PND on FluoroMyelin density [$F(1,25) = 32.240$, $P < .001$], however, this effect was not sex-dependent. Taken together, the observed increases in both MBP expression and compact myelin density indicate accelerated myelination during the postnatal period.

Microglial Activation

To determine whether the observed changes in hippocampal and CC areas and CC myelination were correlated with a neuroinflammatory phenotype, the level of microglial activation in both regions was quantitatively scored as described in the methods (Figure 7a) using a modification of established methods (Hutson *et al.*, 2011). In female hippocampus (Figure 7b), CAPs exposure shifted the microglial phenotype towards the most activated state without altering the total number of microglia [$F(1,16) = 8.798$, $P = .0091$], while these measures were unaffected in males. Interestingly, CAPs exposure caused a statistically significant shift towards an activated microglial phenotype in CC (Figure 7c) of both females [$F(1,15) = 8.739$, $P = .0098$ corresponding to a 25.8% decrease for 3, $F(1,15) = 15.0001$, $P = .0015$ corresponding to a 54.9% increase for 4] and males [$F(1,11) = 6.715$, $p = 0.0251$ for 4], and a decrease in the number of fully ramified, quiescent microglia in both sexes [$F(1,15) = 10.198$, $P = .006$ for females, $F(1,11) = 17.224$, $P = .0016$ for males]. CAPs treatment resulted in a significant 19.5% decrease in the total number of microglia in CC of males [$F(1,11) = 9.212$, $P = .0113$], with a trending decrease in the CAPs-exposed females [$F(1,15) = 3.219$], $P = .09$; Figure 7c], in contrast to hippocampus, where there was no change in the total number of microglia in either sex.

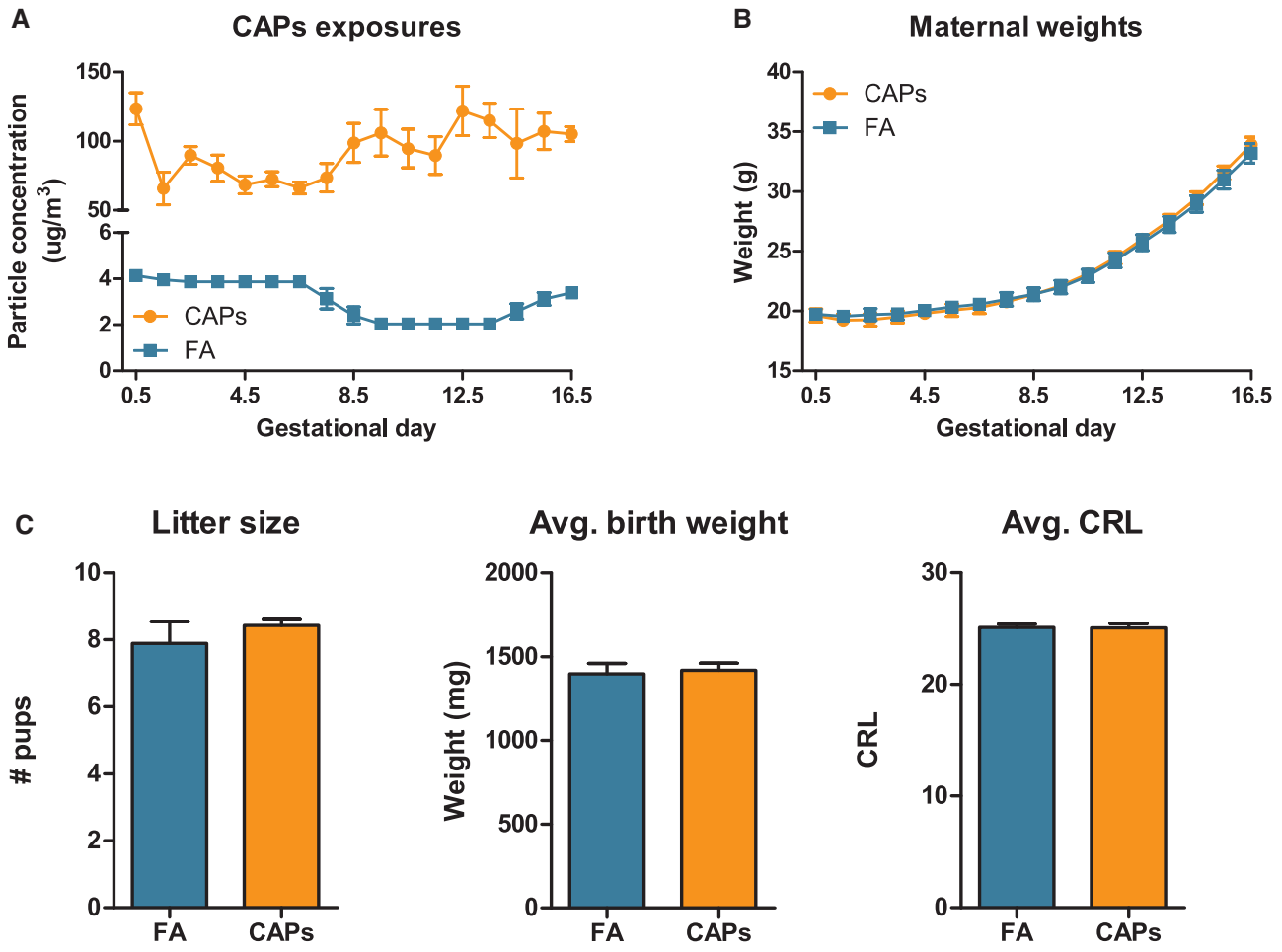

FIG. 1. CAPs exposure during pregnancy does not induce overt maternal toxicity or alter reproductive success. (A) Average CAPs exposure levels were 92.69 ± 19.16 μg/m^3 (mean ± SD; squares) as compared to 3.52 ± 0.87μg/m^3 for FA controls (circles) as determined by weighing particles on pre-weighed Teflon filters. (B) Dam weights (mean ± SEM) were taken daily throughout the course of exposures. (C) Reproductive success was not altered by CAPs exposure, as measured by litter size, birth weights, or crown-rump length at birth. Reproductive success data represent mean ± SEM; N = 16 dams.

Iron Levels in CC

XRF analysis of filters from the CAPs exposure chambers for elevations in elemental particle deposition revealed that ambient iron was elevated approximately 375-fold compared to FA chambers (Figure 8a). Other elements and metals were also elevated in these CAPs exposures relative to FA, particularly sulfur, potassium, manganese, and nickel (Table 1).

To determine whether CAPs-induced microglial activation and hypermyelination in the CC coincides with iron deposition in this region, possibly contributing to the observed hypermyelination phenotype, iron content of CC was first analyzed using Perl's Prussian Blue stain for iron, a well-characterized stain for iron (Perl and Good, 1992), and iron inclusions were quantified in the CC and summed across 3 tissue sections. In female CAPs-exposed offspring, there was a significant 106% increase in iron deposition in the CC (compared to FA controls) that was not present in the male CAPs-treated group (Figure 8b).

Given the increase in CC iron deposition in CAPs treated females and the unusually high baseline iron levels in FA control males, the relative levels of iron were plotted against observed callosal pathologies, i.e. CC area, total microglial number, and MBP density, in order to determine whether these endpoints were significantly correlated and examined separately for each treatment group/gender (Figure 9). FluoroMyelin density was not correlated against iron as both MBP and FluoroMyelin trended similarly. In female CAPs-treated, but not FA-treated offspring, a statistically significant negative relationship between CC iron levels and CC area [$r^2 = 0.5284$, $P = .0309$] and between CC iron levels and total microglial number [$r^2 = 0.3518$, $P = .0272$] was observed. Importantly, CC iron exhibited a statistically significant positive relationship with MBP density [$r^2 = 0.5966$, $p = 0.0418$; Figure 9a], i.e., increased iron levels were associated with increased MBP density in females. CAPs-treated male offspring (Figure 9b) exhibited statistically significant negative relationships between CC iron levels and total microglial number [$r^2 = 0.8093$, $P = .0376$] and between CC iron levels and MBP density [$r^2 = 0.5999$, $P = .0163$], albeit the latter was likely due to an outlying value. There was no statistically significant relationship between CC iron levels and CC area in the CAPs-treated male offspring. Similarly, FA male offspring did not exhibit any statistically significant relationships between CC iron and other CC pathologies.

DISCUSSION

Results from this study demonstrate that gestational CAPs exposure at levels consistent with values commonly measured near California freeway sites (Fruin *et al.*, 2008; Ostro *et al.*, 2010)

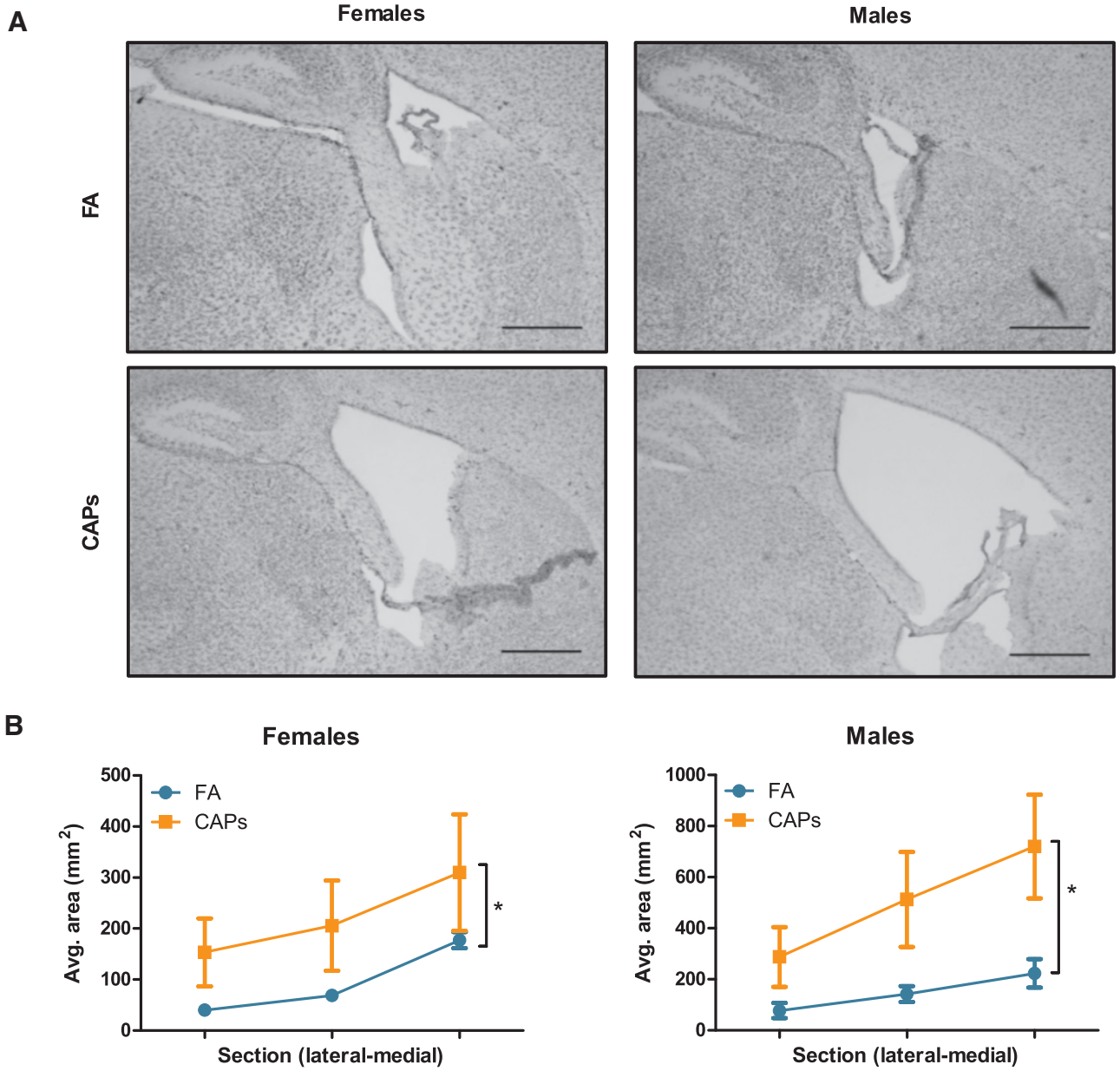

FIG. 2. Prenatal CAPs exposure increases ventricular area in both sexes. Ventricular area was determined by tracing the lateral ventricles. (**A**) Representative micrographs at 10× magnification. Scale bars represent 500 μm distance. (**B**) Gestational CAPs treatment significantly increased quantified lateral to medial ventricular area in both males and females compared to FA controls. Statistical outcome: * = main effect of CAPs across sexes; PND*sex = statistical interaction between PND and sex. Data represent mean ± SEM of 3 serial sections of brain tissue ($N = 6–11$/group).

can produce neuropathological changes. These pathologies include microglial activation and ventriculomegaly, increased size of the CC (the largest white matter tract of the brain and critical to interhemispheric connectivity), along with associated increased and developmentally early expression of myelin basic protein, and reduction in hippocampal size. All pathologies were observed without changes in maternal weight or evaluated adverse reproductive outcomes. These effects were largely similar in males vs. females, whereas elevated levels of iron (a major component of myelin biosynthesis) from the CAPs exposure, increased CC iron levels only in females, and these were significantly correlated with increased myelin density.

In considering fetal brain exposures, placental followed by direct fetal brain translocation of UFP itself seems improbable (Pietroiusti *et al.*, 2013). One likely mechanism for fetal brain exposure includes maternal/placental inflammation. Evidence for the latter comes from *in vivo* studies of gestational exposures to viral or bacterial infectious agents that likewise induce ventriculomegaly, microglial activation, and white matter damage in the brains of offspring by inflammatory mechanisms (Bergeron *et al.*, 2013; Harry *et al.*, 2006; Wang *et al.*, 2006). Further, $PM_{2.5}$ exposure throughout pregnancy has been shown to induce mitochondrial oxidative stress in human maternal blood and fetal umbilical cord blood when sampled at delivery (Grevendonk

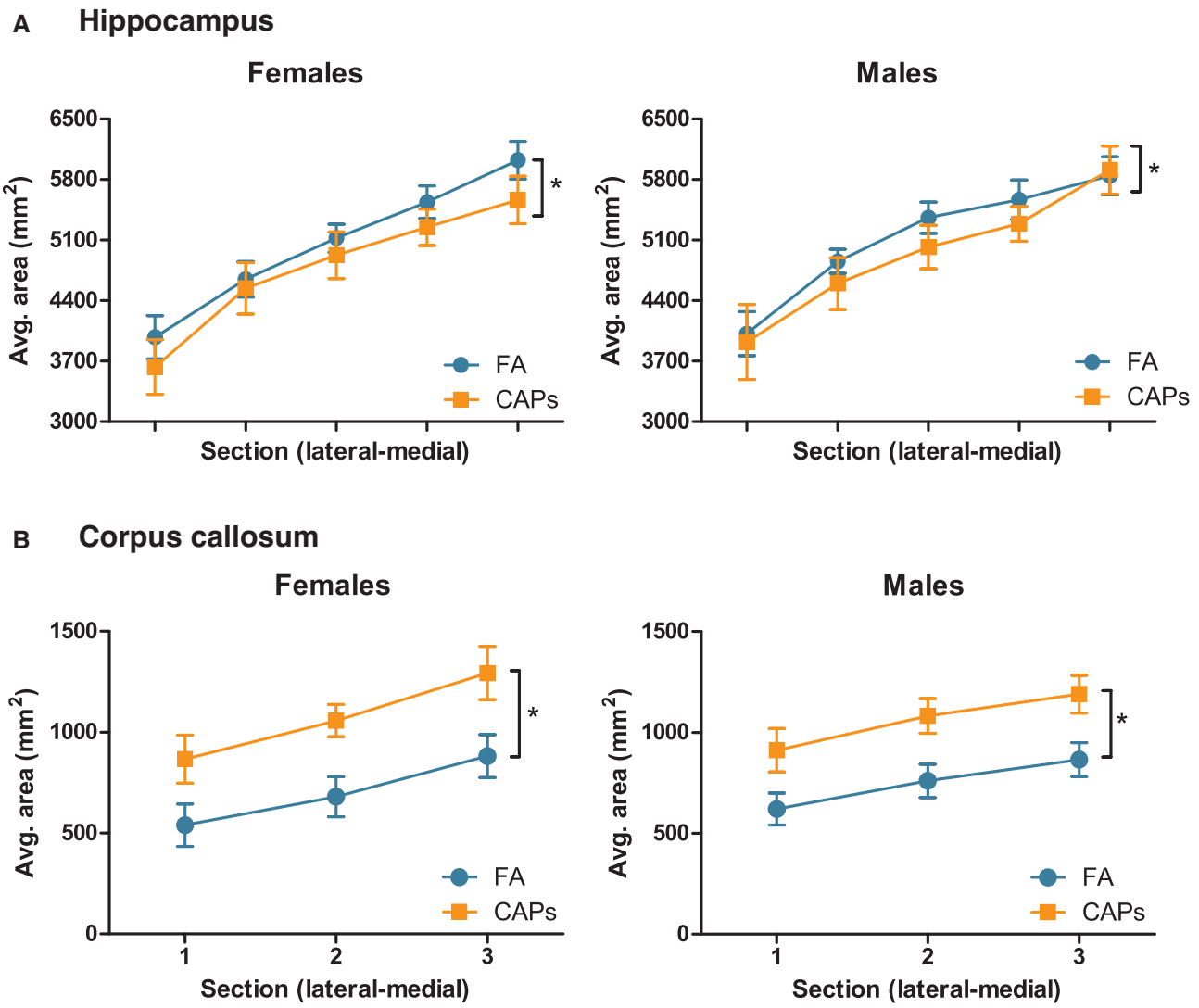

FIG. 3. Prenatal CAPs exposure alters periventricular brain structure size. (**A**) CAPs significantly reduced hippocampal area relative to FA controls and included a main effect of PND and a PND by sex interaction. (**B**) Gestational CAPs significantly increased myelinated area of CC compared to FA controls, with a significant main effect of PND. Statistical outcome: * = main effect of CAPS across sexes. Data represent mean ± SEM of 3–5 serial sections of brain tissue ($N = 6$–11/group).

et al., 2016). In our prior studies at a different exposure site (Rochester, NY), early postnatal UFP CAPs (PNDs 4–7 and 10–13) in mice induced microglial activation and proinflammatory cytokine secretion in the brain, confirming the direct neuroinflammatory properties of such exposures (Allen, et al., 2014a; Allen, et al., 2014c). It is possible that CAPs exposures induced a neuroinflammatory response in the dams, which could, in theory, affect a pregnancy. A separate cohort of pregnant dams exposed using the NYU VACES concentrator showed a mild elevation in striatal microglial activation in the dam brains, but no other pathologies (data not shown). This suggests that any neuroinflammatory dysregulation of the pregnancy, and therefore neurodevelopment, likely has less of an effect compared to systemic maternal and placental inflammation.

In addition, the fetus could be a target of exposure to contaminants adsorbed to particles (Penn *et al.*, 2005) capable of transfer through the placenta and fetal brain barrier. These could include essential nutrients that can also be neurotoxic, such as metals. Iron was found to be elevated in the lung after cigarette smoke PM exposures with corresponding elevations in systemic indicators of iron status (Ghio *et al.*, 2008), and in serum of children who experienced high levels of PM exposure in Mexico City (Calderón-Garcidueñas *et al.*, 2015). Iron is readily transported across the placenta and, given the high levels of iron in our exposures and the increase in iron deposition in the CC of CAPs-treated females, it is possible that iron in our CAPs exposure was able to translocate to the fetal brain (Rao and Georgieff, 2002). Other nanoparticle species have been shown to be capable of placental transfer and accumulation in fetal tissue (Pietroiusti *et al.*, 2013; Semmler-Behnke *et al.*, 2014). However, it remains unclear whether translocation of iron is as a soluble ion bound to transport proteins or the particle itself.

The unexpected observation of increased and developmentally-accelerated myelin expression in CC following gestational CAPs exposure could be related to elevated fetal brain iron exposures. Altered metal homeostasis has long been associated with developmental neurotoxicity, and iron specifically is a key and necessary element for myelin biosynthesis (Connor and Menzies, 1996; Todorich *et al.*, 2009). Characterization of metal content by XRF analysis of filters

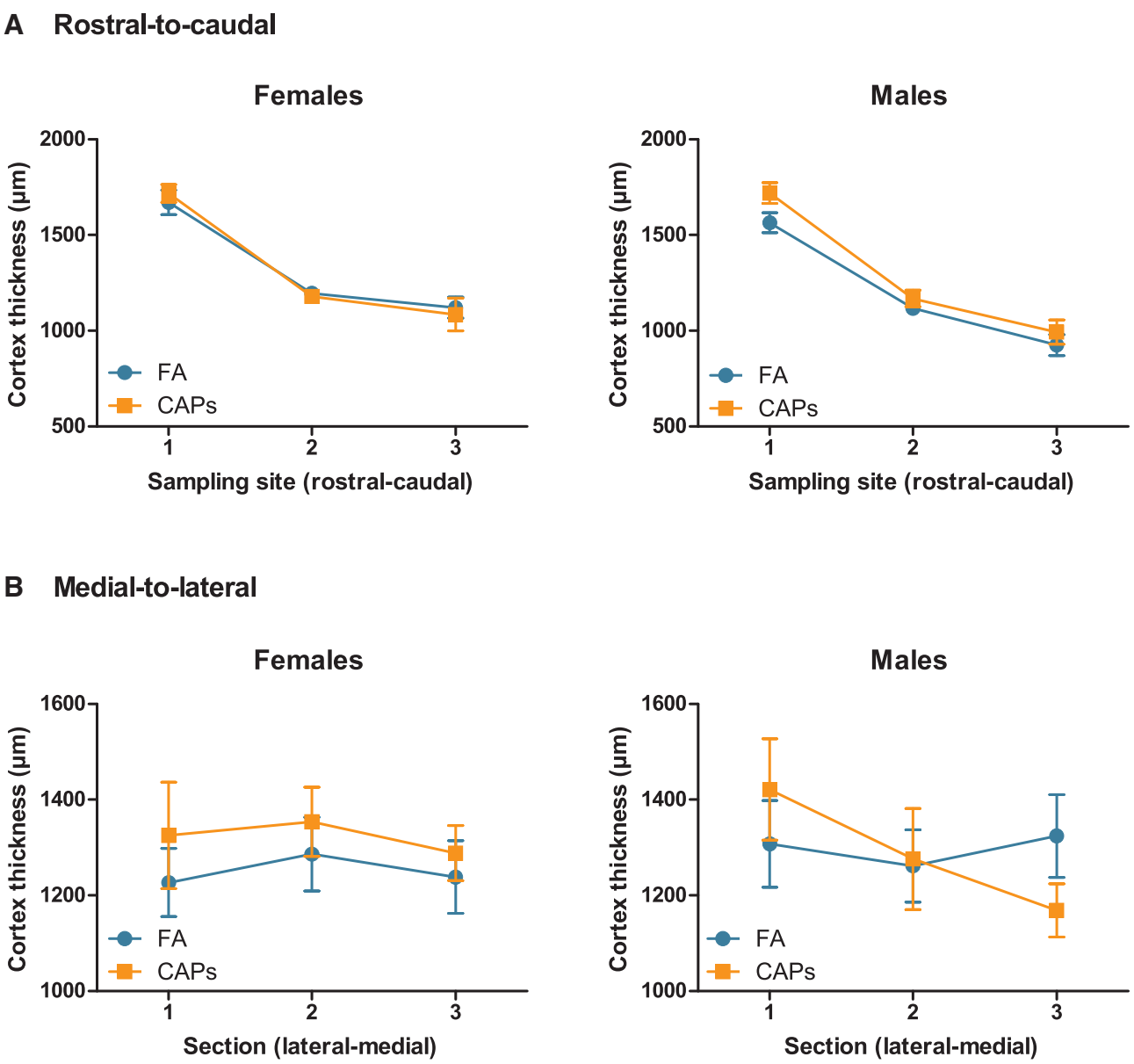

FIG. 4. Prenatal CAPs exposure does not affect frontal cortex thickness in either sex. Cortical thickness was measured by tracing the width of 3 regions of the frontal cortex in 3 sequential tissue sections, denoted on the *x*-axis. (**A**) In the rostral-to-caudal direction, CAPs exposure did not significantly alter cortical thickness. There was a statistically significant effect of sex [$F(1,25) = 4.424$, $P = .0457$, female] for these data. (**B**) Similarly, lateral-to-medial cortical thickness was not altered by prenatal CAPs exposure. Data represent mean ± SEM of 3 serial sections/sampling sites ($N = 6$–11 per group).

collected during our CAPs exposure show iron content to be 375-fold higher than in filtered air (3.8 ± 1.0 FA vs. 1430.1 ± 928.1 ng/m^3 CAPs) with an associated increase in iron deposition in the CC of CAPs-treated females that was significantly correlated with increased myelin density. The apparent sexually dimorphic effect observed here will be discussed further. In relating hypermyelination to disorders of the human brain, this phenotype has been reported in conditions such as Sturge Weber syndrome and hemimegalencephaly (Goldsberry *et al.*, 2011; Pascual-Castroviejo *et al.*, 1993). Moreover, studies show white matter overgrowth in children prior to 4 years of age in children diagnosed with ASD, but reduced white matter maturation at later ages (Ouyang *et al.*, 2016).

During gestation, placental transfer of iron occurs via transferrin receptors, after which it traverses the fetal endothelium to reach the fetal circulation (Gambling *et al.*, 2003). The machinery for this process is established during gestation in rodents, i.e., during the period of CAPs exposures used here, with non-heme iron detectable in choroid plexus epithelial cells by GD14 and in developing axonal tracts of fetal CC by GD19 (Moos, 1995). It has been shown that iron availability can drive the maturation of glial restricted precursors (GRPs) to oligodendrocytes (Morath and Mayer-Pröschel, 2001). A study in mice overexpressing transferrin showed an increase in the synthesis of myelin components in the brain, i.e. MBP, phospholipids, and galactolipids, although this did not lead to alteration of myelin thickness or increased brain iron levels (Saleh *et al.*, 2003). Collectively, such observations suggest a basis for the significant positive association between iron and CC myelin density/area in female CAPs-treated offspring.

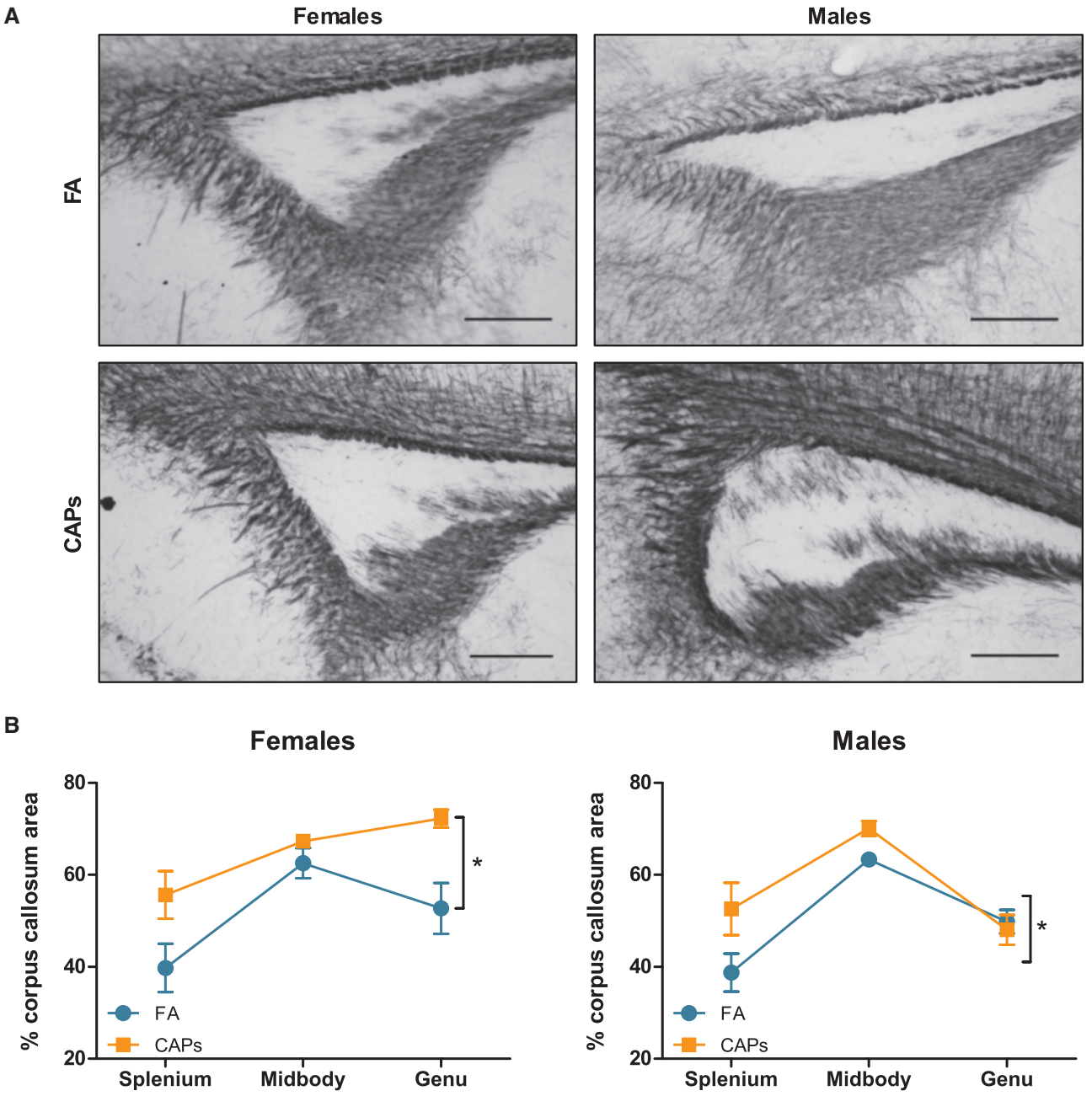

FIG. 5. Prenatal CAPs exposure induces premature increases in myelin expression in of corpus callosum. CAPs significantly increased MBP density across the 3 major regions indicated: genu (rostral portion), midbody (central portion), and splenium (caudal portion). (**A**) Representative micrographs of PND15 splenium at 10X magnification. Scale bars represent 500 μm distance. (**B**) Data is expressed as a percent of CC area positively stained for MBP. Statistical outcome: * = main effect of CAPs across sexes; main effect of PND; PND by sex interaction. Data represent mean ± SEM of 3 serial sections of brain tissue ($N = 6–11$ per group).

CAPs exposure in this study occurred during a developmental period during which oligodendrocyte progenitors proliferate and differentiate into mature, myelinating oligodendrocytes. It is possible that CAPs-generated inflammation and oxidative stress could induce proliferation, leading to a subsequent inappropriate increase in myelinating oligodendrocytes. This was observed in a model of gestational inflammation where pups exhibited brain overgrowth and increased stem cell proliferation after maternal LPS stimulation (Le Belle *et al.*, 2014). Moreover, studies suggest that glial progenitor cells are highly sensitive to changes in their redox balance and might also be a target for CAPs exposure-associated inflammation (Noble *et al.*, 2003). Indeed, further investigation of this hypermyelination phenotype must be considered, including ultrastructural assessment of myelin sheath integrity and quantification of both oligodendrocyte precursors and mature oligodendrocytes.

Despite increases in CC myelination in males, however, there was no corresponding increase in CC iron levels at the time of measurement. Several different reasons for this difference should be considered. Although the interaction of treatment by sex was not statistically significant for myelin expression levels in CC ($P = .10$), the data suggest a somewhat larger elevation in females than in males, suggesting CC iron uptake may be influenced by sex hormones. In support of this,

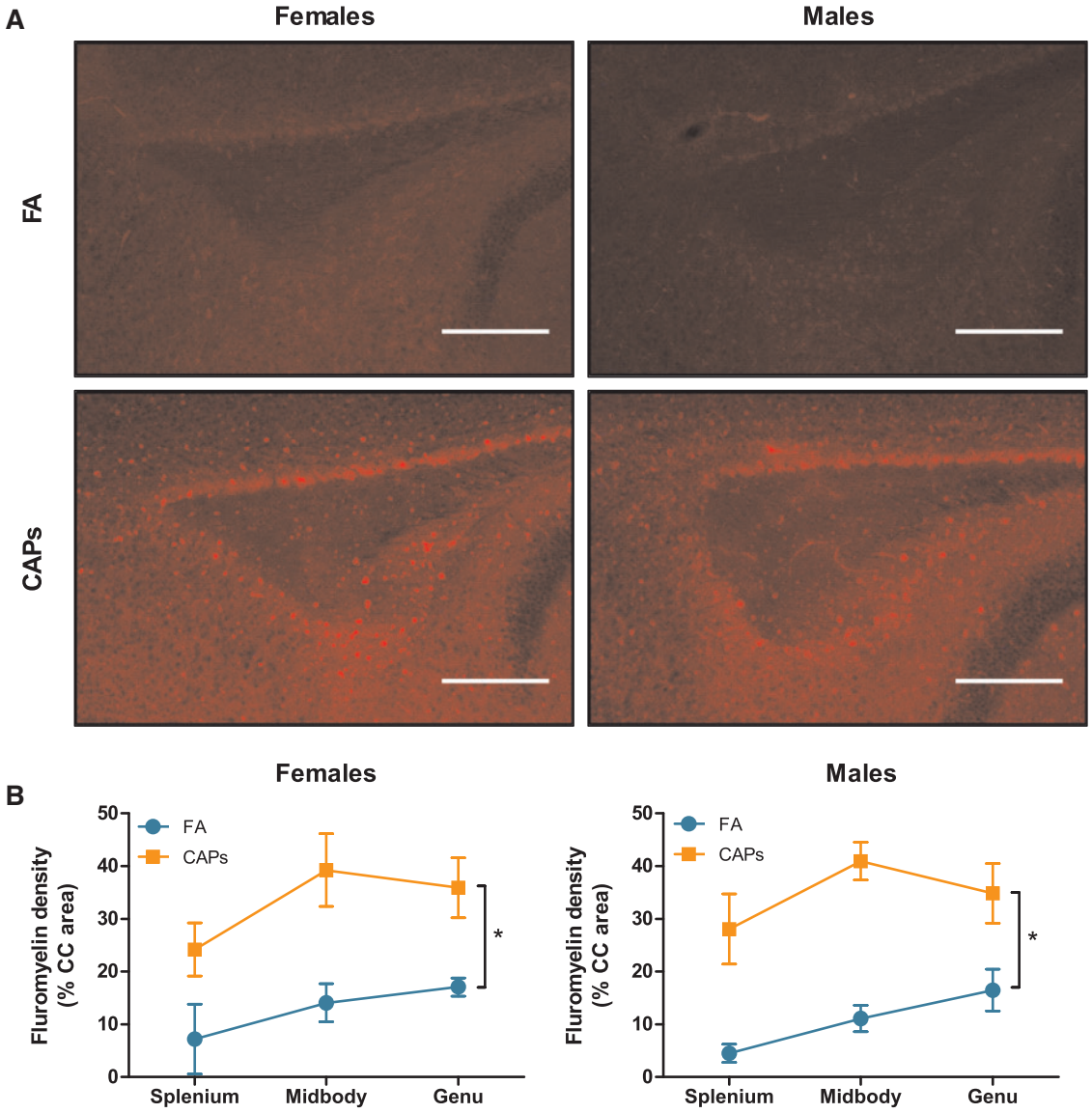

FIG. 6. Prenatal CAPs exposure results in increased presence of compact myelin in the CC. CAPs significantly increased compact myelin, as indicated by FluoroMyelin Red staining density, across the 3 major regions indicated: genu (rostral portion), midbody (central portion), and splenium (caudal portion). (**A**) Representative micrographs of PND15 splenium at 10X magnification. Scale bars represent 500μm distance. B) Data is expressed as a percent of CC area positively stained by FluoroMyelin. Statistical outcome: * = main effect of CAPs across sexes; main effect of PND. Data represent mean ± SEM of 3 serial sections of brain tissue ($N = 6–11$ per group).

iron status has been shown to be sexually dimorphic in both humans and rats (Kong *et al.*, 2014; Zacharski *et al.*, 2000). Estrogen modulates iron homeostasis via controlling the expression of hepcidin, a regulatory hormone that controls uptake, storage, and tissue distribution of iron (Dacks, 2012; Hou *et al.*, 2012). Sex differences in total brain iron have been observed with no corresponding effect of sex on the reduction of myelin in a model of developmental iron deficiency in mice (Kwik-Uribe *et al.*, 2000). In humans, sex differences in serum ferritin and hemoglobin were observed in infants (Domellöf *et al.*, 2002; Tamura *et al.*, 1999) and, additionally, sexually dimorphic brain ferritin iron levels were observed in adults, corresponding with increased risk for neurodegenerative disorders such as Alzheimer's and Parkinson's diseases (Bartzokis *et al.*, 2007). It is thus plausible that sex differences in CC iron observed in this study simply reflect sexually dimorphic regulation of iron homeostasis. It must also be considered that CC hypermyelination is, in fact, not due to elevated iron levels, but rather to other components of the exposure (i.e. other metals) and/or alternate physiological responses to CAPs exposure.

Iron also has the potential to cause oxidative stress, of which lipid peroxidation via free radical products of the Fenton and Haber-Weiss reactions is of particular interest with regard to myelin (Willmore and Triggs, 1991). It is possible that the absence of effects in males relates to the sexual dimorphism in microglial phenotype and expansion at the postnatal age at which these measures were taken (PND 11-15) in mice. Specifically, during the postnatal period, microglia in the male brain are typically both more numerous and more activated compared to females, and thus may be more susceptible to inflammation-based insults (Schwarz and Bilbo, 2012). Therefore, iron exposure may have contributed to a greater loss

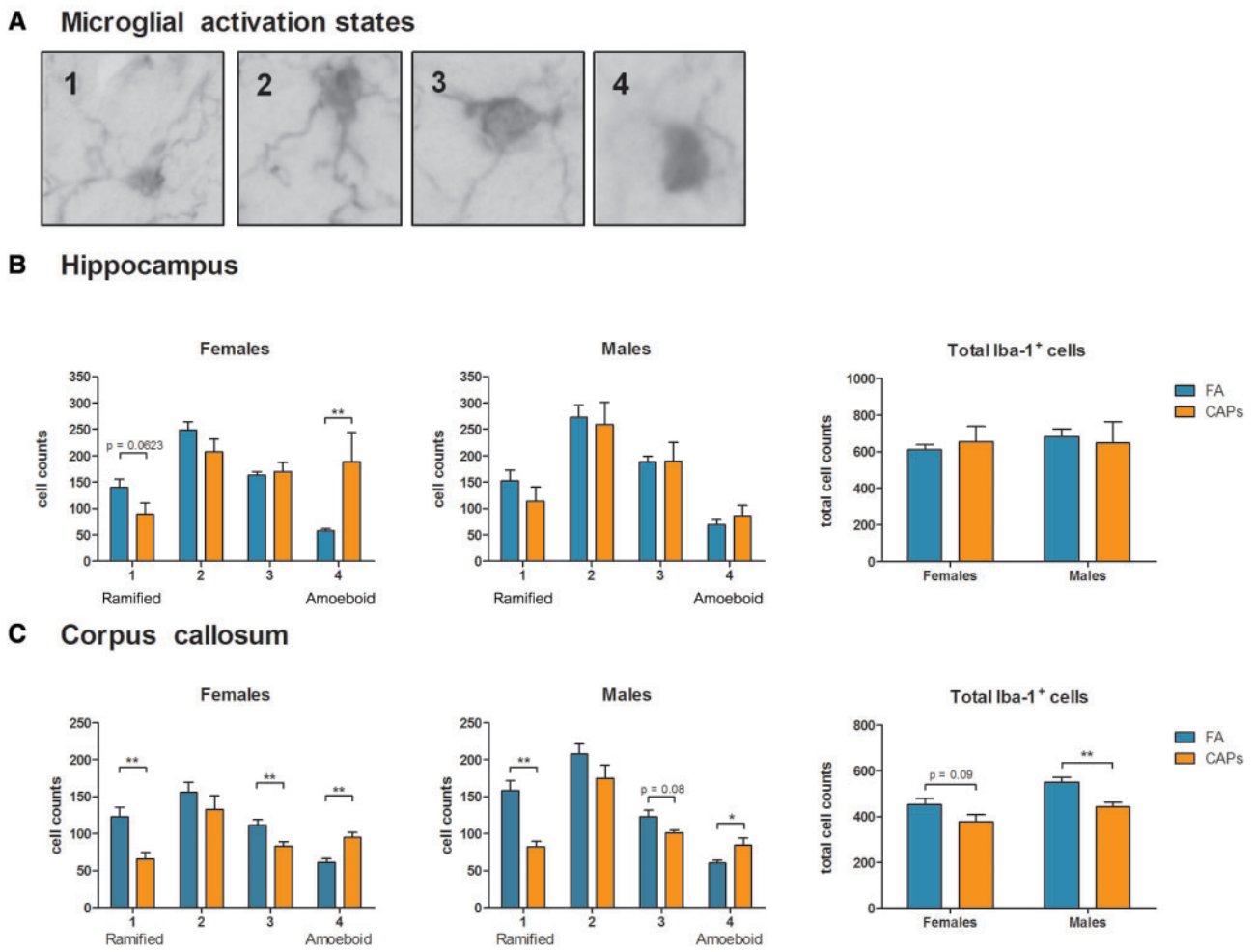

FIG. 7. Prenatal CAPs exposure shifts microglia towards an activated phenotype in a sex- and regionally dependent manner. (**A**) Microglia were assigned a numerical activation state of 1 (quiescent glia with fully ramified morphology), 2 (quiescent microglia with less ramified processes with cell bodies increasing in size), 3 (larger cell body and loss of some, but not all, processes), or 4 (complete loss of ramification and a large, amoeboid cell body). (**B**) Gestational CAPs shifted microglia towards an activated phenotype in hippocampus of females, but not males, without altering the total number of microglia counted. (**C**) Gestational CAPs shifted microglia towards an activated phenotype in CC in both sexes, with a significant corresponding shift away from ramified microglia and significantly decreased the total number of microglia in this region. Data represent mean ± SEM of 3 serial sections of brain tissue ($N = 6$–11 per group). $^{*}P < .05$, $^{**}P < .01$.

of microglia and corresponding decreasing CC iron levels, as activated microglia in a pro-inflammatory environment express iron transport proteins and sequester iron (Mairuae *et al.*, 2011).

An activated microglial phenotype in the presence of iron has been shown to be toxic to oligodendrocytes (Zhang *et al.*, 2006). This would be consistent with the observation that total microglial counts were significantly reduced by CAPs exposure in males, whereas effects were only marginal in females. Conversely, females, with a lower baseline population of microglia, could be unable to efficiently clear excess iron particles that deposit in this region. The Perl's Prussian Blue stain used here only detects iron in the ferric (Fe^{3+}) state and iron present in other molecule-bound forms and valence states may be present (Perl and Good, 1992), providing another possible explanation of the observed sexual dimorphism in CC iron deposition. These differences suggest that sex-specific mechanisms for neurotoxicity of gestational air pollution exposure must be considered and investigated further.

It is important to note that other metal species were also likely elevated by our exposures (Blum *et al.*, 2013) and will ultimately need to be considered for the collective findings, given that any systemic response to CAPs in the pregnant dam begins affecting the embryo almost immediately. As shown in Table 1, elemental copper (Cu), nickel (Ni), manganese (Mn), and lead (Pb) were elevated in CAPs chambers in addition to iron. Elevated copper levels have been reported in the cerebrospinal fluid of patients with Skogholt's disease, which is characterized by central and peripheral nervous system demyelination (Aspli *et al.*, 2015). Copper elevation in the brain is also seen following administration of cuprizone, a widely-used experimental demyelinating agent (Herring and Konradi, 2011; Zatta *et al.*, 2005). In the case of lead, a well-described neurotoxicant (reviewed in (Mason *et al.*, 2014), elevated levels in the brain correspond to impaired oligodendrocyte differentiation and a disruption of myelin integrity (Dabrowska-Bouta *et al.*, 2000; Deng *et al.*, 2001). Limited evidence exists regarding the effects of nickel on oligodendrocyte function or myelin formation. Calderón-Garcidueñas *et al.* (2015) reported a significant correlation between air pollution exposure and increased nickel and antibodies against MBP in the cerebrospinal fluid of children in

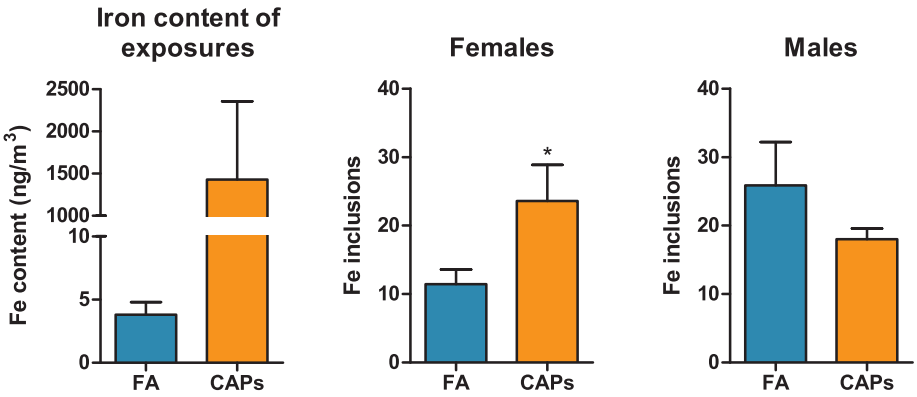

FIG. 8. Prenatal CAPs exposure increases iron deposition in the female CC. Tissue was stained for endogenous iron using Perl's Prussian Blue stain for iron. The total number of iron inclusions was quantified in the CC across 3 sequential tissue sections. (**A**) Iron content of CAPs exposures was determined by XRF (mean ± SD). (**B**) Iron inclusions were significantly increased in the female CC with no significant change in the male CC (mean ± SEM). Data represent mean of 3 serial sections of brain tissue ($N = 6–11$ per group). *$P < .05$ vs. control; #$P < .05$ vs. female FA.

TABLE 1. Elemental X-Ray Fluorescecnce Characterization of Teflon Filters From Ambient Air and Exposure Chambers

Element	Ambient air (ng/m^3)	FA (ng/m^3)	CAPs (ng/m^3)	Fold change from FA
Na	37.2 [± 23.5]	6.0 [± 10.2]	345.0 [± 125.8]	57.5
Mg	10.5 [± 5.0]	5.1 [± 2.8]	117.3 [± 39.0]	23.4
S	594.5 [± 153.1]	6.6 [± 1.6]	4456.3 [± 1039.9]	675.0
K	43.8 [± 6.6]	2.5 [± 0.7]	312.8 [± 70.3]	125.2
Ca	27.3 [± 5.9]	7.6 [± 2.7]	190.3 [± 62.7]	25.0
Mn	4.3 [± 0.1]	0.5 [± 0.1]	50.9 [± 33.9]	101.8
Fe	61.5 [± 28.9]	3.8 [± 1.0]	1430.1 [± 928.1]	376.3
Ni	1.6 [± 0.2]	0.4 [± 0]	123.2 [± 86.1]	307.5
Cu	1.4 [± 0.8]	0 [± 0.1]	40.8 [± 27.8]	40.8
Zn	19.9 [± 13.1]	1.1 [± 1.2]	34.6 [± 11.0]	31.5
Sr	0.1 [± 0.6]	0.1 [± 0.1]	5.9 [± 3.4]	59.0

Values in Ambient, FA, and CAPs colums reperesent mean ± SEM ($N = 7$ filters/atmosphere).

Mexico City, suggesting a link between nickel and CNS immune dysregulation. Evidence supports a minor role for manganese and zinc in oligodendrocyte in myelin function (Bourre *et al.*, 1987), however, given that levels of these elements were not elevated to the extent of iron in CAPs chambers (101.8-fold, 31.5-fold, and 376.3-fold, respectively), it is likely that a greater proportion of observed myelination effects in this study results from iron, assuming myelin effects are the direct result of exposure. That excess myelin is not described as a result of Cu, Ni, Mn, Zn, or Pb exposure does not negate the potential for mixture-related effects, a hypothesis that would require extensive investigation in order to deliniate effects of individual elements (e.g. iron) on myelin versus additive and synergistic effects. Additional constituent pollutants, such as PAHs and gases, must also be considered, however, as current evidence indicates that these toxicants are deleterious for oligodendrocyte differentiation and myelination (Fernández *et al.*, 2010; Solnyshkova and Shakhlamov, 2002).

Changes in other brain development processes likewise warrant examination. In addition to glial expansion and increased myelinating oligodendrocytes, the fetal period involves neuronal differentiation, migration, and synaptogenesis, all of which are facilitated by glia (Rowitch and Kriegstein, 2010). Disruptions in the glial facilitation of neurogenic processes can alter neural fate (Russo *et al.*, 2011), which, along with disruption of myelination and iron homeostasis, has the potential to cause deficits in memory processes and behavioral dysfunction later in life (Bilbo and Schwarz, 2009). Of note, evaluations of the consequences of exposure in this study did not occur until a later period of time, i.e., during postnatal neurodevelopment, which could also mean that some effects could have been subject to repair mechanisms.

Postnatal CAPs exposures produced neuropathology with a striking male bias (Allen, et al., 2014a). Although based on a different CAPs exposure than that used for the studies here, i.e., ambient concentrated UFP from Rochester, NY (Allen *et al.*, 2014a, 2015) vs. concentrated ambient fine/UFP particle exposures from Tuxedo, NY (Maciejczyk *et al.*, 2005), and therefore likely different PM constituents at different concentrations, sex differences in this study were not prominent in response to gestational exposures. In contrast to postnatal CAPs exposure studies by Allen et. al, females in this study were affected by gestational CAPs as much, and in some cases more (i.e., hippocampal microglial activation), than males, confirming the importance of timing of exposure to outcome. Gestational CAPs exposure occur prior to the period of the major sexual differentiation of rodent brain (Chung and Auger, 2013), whereas postnatal CAPs exposures (Allen *et al.*, 2013, 2014a, 2014b, 2014c, 2015) occurred during a period in which brain colonizing microglia numbers and activation state differ considerably by sex, with male mice have greater numbers of and more activated microglia than females (Schwarz and Bilbo, 2012), a phenotype

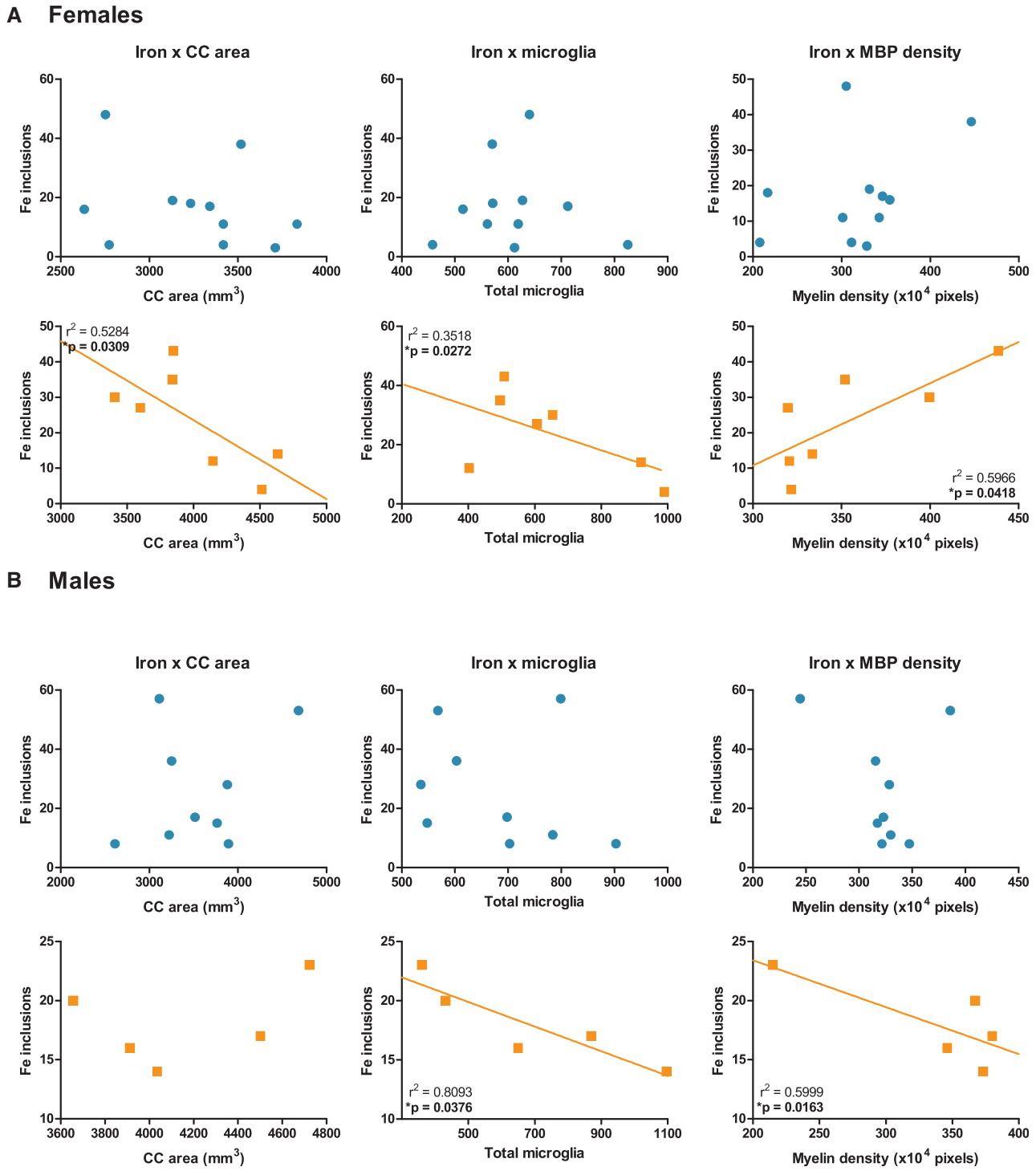

FIG. 9. Correlative relationships between CC iron levels and CC area, CC microglia, and myelin density. Corpus callosum area, total microglial number, and myelin density are plotted against total iron inclusions for both FA (circles; first and third rows) and CAPs (squares; second and fourth rows) treated offspring. Each data point represents an individual animal. (**A**) Female CAPs treated offspring showed statistically significant ($P < .05$) correlation between callosal iron levels and CC area, total microglia, and MBP density. No significant correlation was observed between CC iron and any endpoint in FA treated females. (**B**) Male CAPs treated offspring had statistically significant ($P < .05$) correlations between CC iron, total microglia, and MBP density, but no significant correlation was observed between CC iron and CC area. No significant correlation was observed between CC iron and any endpoint in FA treated males. Data represent mean of 3 serial sections of brain tissue ($N = 6–11$ per group).

likely increasing vulnerability to further microglial activation. The fact that such normal sex-related differences typically seen at PND 11–15 were not apparent following gestational CAPs exposure, i.e., there were no sex-related differences in the total number of microglia counted in either hippocampus or CC, suggests that gestational CAPs exposure may have disrupted the normal trajectory and sexual dimorphism of microglial colonization and expansion. Given the complex

functional relationships between iron status, microglial activation, and oligodendrocyte survival, further studies will be required to understand the mechanisms of these sex-based differences in response to gestational and postnatal PM exposures.

This study provides further support for the considerable experimental and epidemiologcal data indicating the developmental vulnerability of the brain to airborne particulate pollutants. The neurodevelopmental alterations observed here are of particular translational significance as some of these neuropathological consequences are hallmarks of neurodevelopmental disorders in children. Ventriculomegaly, a clinical indicator of white matter damage leading to brain interhemispheric disconnectivity, characterizes periventricular leukomalacia (white matter damage of prematurity), which occurs in 5–10% of low or extremely low for birth weight (LBW) babies (Volpe, 2003). The similarity is notable given reports that gestational exposures to airborne pollutants, including UFP, increase preterm birth and LBW (Shah and Balkhair, 2011). Ventriculomegaly also occurs in schizophrenia and is associated with a higher risk for ASD diagnosis (Movsas *et al.*, 2013; Sanfilipo *et al.*, 2000). Both disorders also include white matter damage (Abdel Razek *et al.*, 2013; Li *et al.*, 2009), and both have been linked to prematurity and LBW (Abel *et al.*, 2010; Schieve *et al.*, 2015). Further, early white matter overgrowth appears to be characteristic of ASD (Ben Bashat *et al.*, 2007; Ouyang, et al., 2016). These findings also highlight the role of air pollution in altering neuroinflammation states during critical windows of sexually dimorphic neurodevelopment.

In contrast to the differences in outcomes in response to postnatal (Allen *et al.*, 2013, 2014a, 2014b, 2014c, 2015) vs. gestational exposures (this study), both exposures produced ventriculomegaly, altered brain white matter and produced microglial activation. This occurred despite the fact that gestational $PM_{2.5}$ exposure was imposed using the VACES system at NYU (Tuxedo Park), while postnatal exposures were accomplished using the HUCAPS system at the University of Rochester Medical School in Rochester NY. This study and previous study produced different myelination phenotypes, which may be a function of timing of exposures, i.e. gestational (1st and 2nd trimester human equivalent) vs. postnatal (3rd trimester human equivalent) exposures, and/or magnitude and composition of exposures. Further study is needed to delineate the effects of these factors with respect to developmental neuropathology. Considered together, these findings suggest mechanisms arising from common elements of such exposures. Further, these data demonstrate the continuing need for regulation of anthropogenic PM emissions, specifically of the more toxic fine and ultrafine particles.

ACKNOWLEDGMENTS

The authors declare no competing financial interests.

FUNDING

This work was supported by the National Institutes of Environmental Health Sciences [grant numbers P30 ES001247 and R01 ES025541 to D.A.C.-S.; T32 ES07026 (B. P. Lawrence), and P30 ES000260; M. Costa, PI], and March of Dimes (21-F12-13) to J.T.Z.

REFERENCES

Abdel Razek, A., Mazroa, J., and Baz, H. (2013). Assessment of white matter integrity of autistic preschool children with diffusion weighted mr imaging. *Brain Dev.* **36(1)**, 28–34.

Abel, K. M., Wicks, S., Susser, E. S., Dalman, C., Pedersen, M. G., Mortensen, P. B., and Webb, R. T. (2010). Birth weight, schizophrenia, and adult mental disorder: is risk confined to the smallest babies?. *Arch. Gen. Psychiatry* **67**, 923–930.

Adar, S. D., Filigrana, P. A., Clements, N., and Peel, J. L. (2014). Ambient coarse particulate matter and human health: a systematic review and meta-analysis. *Curr. Environ. Health. Rep.* **1**, 258–274.

Allen, J. L., Conrad, K., Oberdörster, G., Johnston, C. J., Sleezer, B., and Cory-Slechta, D. A. (2013). Developmental exposure to concentrated ambient particles and preference for immediate reward in mice. *Environ. Health Perspect.* **121**, 32–38.

Allen, J. L., Liu, X., Pelkowski, S., Palmer, B., Conrad, K., Oberdörster, G., Weston, D., Mayer-Pröschel, M., and Cory-Slechta, D. A. (2014a). Early postnatal exposure to ultrafine particulate matter air pollution: Persistent ventriculomegaly, neurochemical disruption, and glial activation preferentially in male mice. *Environ. Health Perspect.* **122**, 939–945.

Allen, J. L., Liu, X., Weston, D., Conrad, K., Oberdörster, G., and Cory-Slechta, D. A. (2014b). Consequences of developmental exposure to concentrated ambient ultrafine particle air pollution combined with the adult paraquat and maneb model of the parkinson's disease phenotype in male mice. *Neurotoxicology* **41**, 80–88.

Allen, J. L., Liu, X., Weston, D., Prince, L., Oberdörster, G., Finkelstein, J. N., Johnston, C. J., and Cory-Slechta, D. A. (2014c). Developmental exposure to concentrated ambient ultrafine particulate matter air pollution in mice results in persistent and sex-dependent behavioral neurotoxicity and glial activation. *Toxicol. Sci* **140**, 160–178.

Allen, J. L., Oberdorster, G., Morris-Schaffer, K., Wong, C., Klocke, C., Sobolewski, M., Conrad, K., Mayer-Proschel, M., and Cory-Slechta, D. A. (2015). Developmental neurotoxicity of inhaled ambient ultrafine particle air pollution: Parallels with neuropathological and behavioral features of autism and other neurodevelopmental disorders. *Neurotoxicology* doi: 10.1016/j.neuro.2015.12.014.

Aspli, K. T., Flaten, T. P., Roos, P. M., Holmøy, T., Skogholt, J. H., and Aaseth, J. (2015). Iron and copper in progressive demyelination–new lessons from skogholt's disease. *Journal of Trace Elements in Medicine and Biology: Organ of the Society for Minerals and Trace Elements (GMS)* **31**, 183–187.

Bandeira, F., Lent, R., and Herculano-Houzel, S. (2009). Changing numbers of neuronal and non-neuronal cells underlie postnatal brain growth in the rat. *Proc. Natl. Acad. Sci. U. S. A* **106**, 14108–14113.

Bartzokis, G., Tishler, T. A., Lu, P. H., Villablanca, P., Altshuler, L. L., Carter, M., Huang, D., Edwards, N., and Mintz, J. (2007). Brain ferritin iron may influence age- and gender-related risks of neurodegeneration. *Neurobiol. Aging* **28**, 414–423.

Bell, M. L., Ebisu, K., Peng, R. D., Samet, J. M., and Dominici, F. (2009). Hospital admissions and chemical composition of fine particle air pollution. *Am. J. Respir. Crit. Care Med.* **179**, 1115–1120.

Ben Bashat, D., Kronfeld-Duenias, V., Zachor, D. A., Ekstein, P. M., Hendler, T., Tarrasch, R., Even, A., Levy, Y., and Ben Sira, L. (2007). Accelerated maturation of white matter in young children with autism: A high b value DWI study. *Neuroimage* **37**, 40–47.

Bergeron, J. D., Deslauriers, J., Grignon, S., Fortier, L. C., Lepage, M., Stroh, T., Poyart, C., and Sebire, G. (2013). White matter injury and autistic-like behavior predominantly affecting male rat offspring exposed to group b streptococcal maternal inflammation. *Dev. Neurosci* **35**, 504–515.

Bilbo, S. D., and Schwarz, J. M. (2009). Early-life programming of later-life brain and behavior: A critical role for the immune system. *Front. Behav. Neurosci* **3**, 14.

Block, M. L., and Calderón-Garcidueñas, L. (2009). Air pollution: mechanisms of neuroinflammation and cns disease. *Trends Neurosci* **32**, 506–516.

Blum, J. L., Chen, L. C., and Zelikoff, J. T. (2013). Inhalation of concentrated ambient particulate matter by pregnant mice leads to adverse obstetric outcomes associated with particular exposure windows. *The Toxicologist* .

Bourre, J. M., Cloez, I., Galliot, M., Buisine, A., Dumont, O., Piciotti, M., Prouillet, F., and Bourdon, R. (1987). Occurrence of manganese, copper and zinc in myelin. Alterations in the peripheral nervous system of dysmyelinating trembler mutant are at variance with brain mutants (quaking and shiverer). *Neurochem. Int.* **10**, 281–286.

Bresgen, N., and Eckl, P. M. (2015). Oxidative stress and the homeodynamics of iron metabolism. *Biomolecules* **5**, 808–847.

Calderón-Garcidueñas, L., Vojdani, A., Blaurock-Busch, E., Busch, Y., Friedle, A., Franco-Lira, M., Sarathi-Mukherjee, P., Martínez-Aguirre, X., Park, S. B., Torres-Jardón, R., *et al.* (2015). Air pollution and children: Neural and tight junction antibodies and combustion metals, the role of barrier breakdown and brain immunity in neurodegeneration. *J. Alzheimer's Dis.* **43**, 1039–1058.

Cherry, J. D., Olschowka, J. A., and O'Banion, M. K. (2014). Neuroinflammation and m2 microglia: The good, the bad, and the inflamed. *J. Neuroinflammation* **11**, 98.

Chung, W. C. J., and Auger, A. P. (2013). Gender differences in neurodevelopment and epigenetics. *Pfluegers Arch./Eur. J. Physiol.* **465**, 573–584.

Connor, J. R., and Menzies, S. L. (1996). Relationship of iron to oligodendrocytes and myelination. *Glia* **17**, 83–93.

Dabrowska-Bouta, B., Sulkowski, G., Walski, M., Struzyńska, L., Lenkiewicz, A., and Rafałowska, U. (2000). Acute lead intoxication in vivo affects myelin membrane morphology and cnpase activity. *Exp. Toxicol. Pathol.* **52**, 257–263.

Dacks, P. A. (2012). Estrogens iron out the details: A novel direct pathway for estrogen control of iron homeostasis. *Endocrinology* **153**, 2942–2944.

de Lacy, N., and King, B. H. (2013). Revisiting the relationship between autism and schizophrenia: Toward an integrated neurobiology. *Annu. Rev. Clin. Psychol.* **9**, 555–587.

Deng, W., McKinnon, R. D., and Poretz, R. D. (2001). Lead exposure delays the differentiation of oligodendroglial progenitors in vitro. *Toxicol. Appl. Pharmacol.* **174**, 235–244.

Domellöf, M., Lönnerdal, B., Dewey, K. G., Cohen, R. J., Rivera, L. L., and Hernell, O. (2002). Sex differences in iron status during infancy. *Pediatrics* **110**, 545–552.

Fernández, M., Paradisi, M., D'Intino, G., Del Vecchio, G., Sivilia, S., Giardino, L., and Calzà, L. (2010). A single prenatal exposure to the endocrine disruptor 2,3,7,8-tetrachlorodibenzo-p-dioxin alters developmental myelination and remyelination potential in the rat brain. *J. Neurochem.* **115**, 897–909.

Franklin, K. B. J., and Paxinos, G. (2007). *The mouse brain in stereotaxic coordinates*. 3rd edn. Elsevier Inc., New York.

Fruin, S., Westerdahl, D., Sax, T., Sioutas, C., and Fine, P. M. (2008). Measurements and predictors of on-road ultrafine particle concentrations and associated pollutants in los angeles. *Atmos. Environ.* **42**, 207–219.

Fujii, T., Hayashi, S., Hogg, J. C., Vincent, R., and Van Eeden, S. F. (2001). Particulate matter induces cytokine expression in human bronchial epithelial cells. *Am. J. Respir. Cell Mol. Biol.* **25**, 265–271.

Gambling, L., Danzeisen, R., Fosset, C., Andersen, H. S., Dunford, S., and Srai, S. K. and HJ, M. C. (2003). Iron and copper interactions in development and the effect on pregnancy outcome. *J. Nutr.* **133(5 Suppl 1)**, 1554S–1556S.

Ghio, A. J., Hilborn, E. D., Stonehuerner, J. G., Dailey, L. A., Carter, J. D., Richards, J. H., Crissman, K. M., Foronjy, R. F., Uyeminami, D. L., and Pinkerton, K. E. (2008). Particulate matter in cigarette smoke alters iron homeostasis to produce a biological effect. *Am. J. Respir. Crit. Care Med.* **178**, 1130–1138.

Goldsberry, G., Mitra, D., MacDonald, D., and Patay, Z. (2011). Accelerated myelination with motor system involvement in a neonate with immediate postnatal onset of seizures and hemimegalencephaly. *Epilepsy Behav.* **22**, 391–394.

Grevendonk, L., Janssen, B. G., Vanpoucke, C., Lefebvre, W., Hoxha, M., Bollati, V., and Nawrot, T. S. (2016). Mitochondrial oxidative DNA damage and exposure to particulate air pollution in mother-newborn pairs. *Environ. Health* **15**, 10.

Harry, G. J., Lawler, C., and Brunssen, S. H. (2006). Maternal infection and white matter toxicity. *Neurotoxicology* **27**, 658–670.

Herring, N. R., and Konradi, C. (2011). Myelin, copper, and the cuprizone model of schizophrenia. *Frontiers in Bioscience (Scholar Edition)* **3**, 23–40.

Hou, Y., Zhang, S., Wang, L., Li, J., Qu, G., He, J., Rong, H., Ji, H., and Liu, S. (2012). Estrogen regulates iron homeostasis through governing hepatic hepcidin expression via an estrogen response element. **511**, 398–403.

Hutson, C. B., Lazo, C. R., Mortazavi, F., Giza, C. C., Hovda, D., and Chesselet, M. F. (2011). Traumatic brain injury in adult rats causes progressive nigrostriatal dopaminergic cell loss and enhanced vulnerability to the pesticide paraquat. *J. Neurotrauma.* **28**, 1783–1801.

Kalkbrenner, A. E., Windham, G. C., Serre, M. L., Akita, Y., Wang, X., Hoffman, K., Thayer, B. P., and Daniels, J. L. (2015). Particulate matter exposure, prenatal and postnatal windows of susceptibility, and autism spectrum disorders. *Epidemiology* **26**, 30–42.

Kambe, T., Weaver, B. P., and Andrews, G. K. (2008). The genetics of essential metal homeostasis during development. *Genesis* **46**, 214–228.

Kelly, F. J., and Fussell, J. C. (2015). Linking ambient particulate matter pollution effects with oxidative biology and immune responses. *Ann. N. Y. Acad. Sci.* **1340**, 84–94.

Kim, S., Jaques, P. A., Chang, M., Froines, J. R., and Sioutas, C. (2001). Versatile aerosol concentration enrichment system (vaces) for simultaneous in vivo and in vitro evaluation of toxic effects of ultrafine, fine and coarse ambient particles part i: Development and laboratory characterization. *J. Aerosol Sci.* **32**, 1281–1297.

Kong, W. N., Niu, Q. M., Ge, L., Zhang, N., Yan, S. F., Chen, W. B., Chang, Y. Z., and Zhao, S. E. (2014). Sex differences in iron status and hepcidin expression in rats. *Biol. Trace Elem. Res.* **160**, 258–267.

Kwik-Uribe, C. L., Gietzen, D., German, J. B., Golub, M. S., and Keen, C. L. (2000). Chronic marginal iron intakes during early development in mice result in persistent changes in dopamine metabolism and myelin composition. *J. Nutr.* **130**, 2821–2830.

Le Belle, J. E., Sperry, J., Ngo, A., Ghochani, Y., Laks, D. R., Lopez-Aranda, M., Silva, A. J., and Kornblum, H. I. (2014). Maternal inflammation contributes to brain overgrowth and autism-associated behaviors through altered redox signaling in stem and progenitor cells. *Stem Cell Reports* **3**, 725–734.

Lelieveld, J., Evans, J. S., Fnais, M., Giannadaki, D., and Pozzer, A. (2015). The contribution of outdoor air pollution sources to premature mortality on a global scale. *Nature* **525**, 367–371.

Li, Q., Cheung, C., Wei, R., Hui, E. S., Feldon, J., Meyer, U., Chung, S., Chua, S. E., Sham, P. C., Wu, E. X., *et al.* (2009). Prenatal immune challenge is an environmental risk factor for brain and behavior change relevant to schizophrenia: Evidence from mri in a mouse model. *PLoS One* **4**, e6354.

Maciejczyk, P., Zhong, M., Li, Q., Xiong, J., Nadziejko, C., and Chen, L. C. (2005). Effects of subchronic exposures to concentrated ambient particles (caps) in mice. Ii. The design of a caps exposure system for biometric telemetry monitoring. *Inhal. Toxicol* **17**, 189–197.

Mairuae, N., Connor, J. R., and Cheepsunthorn, P. (2011). Increased cellular iron levels affect matrix metalloproteinase expression and phagocytosis in activated microglia. *Neurosci. Lett.* **500**, 36–40.

Mason, L. H., Harp, J. P., and Han, D. Y. (2014). Pb neurotoxicity: neuropsychological effects of lead toxicity. *BioMed. Res. Int.* **2014**, 840547–840547.

McQueen, D. S., Donaldson, K., Bond, S. M., McNeilly, J. D., Newman, S., Barton, N. J., and Duffin, R. (2007). Bilateral vagotomy or atropine pre-treatment reduces experimental diesel-soot induced lung inflammation. *Toxicol. Appl. Pharmacol.* **219**, 62–71.

Meyer, U., Feldon, J., and Dammann, O. (2011). Schizophrenia and autism: Both shared and disorder-specific pathogenesis via perinatal inflammation? *Pediatr. Res.* **69**, 26R–33R.

Moos, T. (1995). Developmental profile of non-heme iron distribution in the rat brain during ontogenesis. *Brain Res. Dev. Brain Res.* **87**, 203–213.

Morath, D. J., and Mayer-Pröschel, M. (2001). Iron modulates the differentiation of a distinct population of glial precursor cells into oligodendrocytes. *Dev. Biol.* **237**, 232–243.

Movsas, T. Z., Pinto-Martin, J. A., Whitaker, A. H., Feldman, J. F., Lorenz, J. M., Korzeniewski, S. J., Levy, S. E., and Paneth, N. (2013). Autism spectrum disorder is associated with ventricular enlargement in a low birth weight population. *J. Pediatr.* **163**(1), 73–78.

Mumaw, C. L., Levesque, S., McGraw, C., Robertson, S., Lucas, S., Stafflinger, J. E., Campen, M. J., Hall, P., Norenberg, J. P., Anderson, T., *et al.* (2016). Microglial priming through the lung-brain axis: the role of air pollution-induced circulating factors. *FASEB J* **30**, 1880–1891.

Noble, M., Smith, J., Power, J., and Mayer-Proschel, M. (2003). Redox state as a central modulator of precursor cell function. *Ann. N. Y. Acad. Sci.* **991**, 251–271.

Oberdörster, G. (2000). Toxicology of ultrafine particles: In vivo studies. *Philos. T. Roy. Soc. A* **358**, 2719–2740.

Oberdorster, G., Elder, A., and Rinderknecht, A. (2009). Nanoparticles and the brain: Cause for concern?. *J. Nanosci. Nanotechnol.* **9**, 4996–5007.

Oberdorster, G., Sharp, Z., Atudorei, V., Elder, A., Gelein, R., Kreyling, W., and Cox, C. (2004). Translocation of inhaled ultrafine particles to the brain. *Inhal. Toxicol.* **16**, 437–445.

Oberdörster, G., Sharp, Z., Atudorei, V., Elder, A., Gelein, R., Kreyling, W., and Cox, C. (2004). Translocation of inhaled ultrafine particles to the brain. *Inhal. Toxicol.* **16**, 437–445.

Ostro, B., Lipsett, M., Reynolds, P., Goldberg, D., Hertz, A., Garcia, C., Henderson, K. D., and Bernstein, L. (2010). Long-term exposure to constituents of fine particulate air pollution and mortality: Results from the california teachers study. *Environ. Health Perspect.* **118**, 363–369.

Ouyang, M., Cheng, H., Mishra, V., Gong, G., Mosconi, M. W., Sweeney, J., Peng, Y., and Huang, H. (2016). Atypical age-dependent effects of autism on white matter microstructure in children of 2-7 years. *Hum. Brain Mapp.* **37**, 819–832.

Pascual-Castroviejo, I., Diaz-Gonzalez, C., Garcia-Melian, R. M., Gonzalez-Casado, I., and Munoz-Hiraldo, E. (1993). Sturge-weber syndrome: Study of 40 patients. *Pediatr. Neurol.* **9**, 283–288.

Penn, A., Murphy, G., Barker, S., Henk, W., and Penn, L. (2005). Combustion-derived ultrafine particles transport organic toxicants to target respiratory cells. *Environ. Health Perspect.* **113**, 956–963.

Perl, D. P., and Good, P. F. (1992). Comparative techniques for determining cellular iron distribution in brain tissues. *Ann. Neurol.* **32**, S76–S81.

Pietroiusti, A., Campagnolo, L., and Fadeel, B. (2013). Interactions of engineered nanoparticles with organs protected by internal biological barriers. *Small* **9**, 1557–1572.

Radlowski, E. C., and Johnson, R. W. (2013). Perinatal iron deficiency and neurocognitive development. *Front. Hum. Neurosci.* **7**, 585–585.

Rao, R., and Georgieff, M. K. (2002). Perinatal aspects of iron metabolism. *Acta Paediatr. Suppl.* **91**, 124–129.

Rice, D., and Barone, S. (2000). Critical periods of vulnerability for the developing nervous system: Evidence from humans and animal models. *Environ. Health Perspect.* **108 Suppl**, 511–533.

Rowitch, D. H., and Kriegstein, A. R. (2010). Developmental genetics of vertebrate glial-cell specification. *Nature* **468**, 214–222.

Russo, I., Barlati, S., and Bosetti, F. (2011). Effects of neuroinflammation on the regenerative capacity of brain stem cells. *J. Neurochem.* **116**, 947–956.

Saleh, M. C., Espinosa de los Monteros, A., de Arriba Zerpa, G. A., Fontaine, I., Piaud, O., Djordjijevic, D., Baroukh, N., Garcia Otin, A. L., Ortiz, E., Lewis, S., *et al.* (2003). Myelination and motor coordination are increased in transferrin transgenic mice. *J. Neurosci. Res.* **72**, 587–594.

Sanfilipo, M., Lafargue, T., Arena, L., Rusinek, H., Kushner, K., Lautin, A., Loneragan, C., Vaid, G., Rotrosen, J., and Wolkin, A. (2000). Fine volumetric analysis of the cerebral ventricular system in schizophrenia: Further evidence for multifocal mild to moderate enlargement. *Schizophr. Bull.* **26**, 201–216.

Schieve, L. A., Clayton, H. B., Durkin, M. S., Wingate, M. S., and Drews-Botsch, C. (2015). Comparison of perinatal risk factors associated with autism spectrum disorder (asd), intellectual disability (id), and co-occurring asd and id. *J. Autism Dev. Disord.* **45**, 2361–2372.

Schwarz, J. M., and Bilbo, S. D. (2012). Sex, glia, and development: Interactions in health and disease. *Horm. Behav.* **62**, 243–253.

Semmler-Behnke, M., Lipka, J., Wenk, A., Hirn, S., Schäffler, M., Tian, F., Schmid, G., Oberdörster, G., and Kreyling, W. G. (2014). Size dependent translocation and fetal accumulation of gold nanoparticles from maternal blood in the rat. *Part. Fibre Toxicol.* **11**, 33.

Shah, P. S., and Balkhair, T. (2011). Air pollution and birth outcomes: A systematic review. *Environ. Int.* **37**, 498–516.

Siddique, S., Banerjee, M., Ray, M. R., and Lahiri, T. (2011). Attention-deficit hyperactivity disorder in children chronically exposed to high level of vehicular pollution. *Eur. J. Pediatr*. **170**, 923–929.

Solnyshkova, T. G., and Shakhlamov, V. A. (2002). Ultrastructural and morphometric characteristics of nerve cells and myelinated fibers in the cerebral cortex after chronic exposure to natural gas containing hydrogen sulfide in low concentrations. *Bull. Exp. Biol. Med*. **134**, 411–413.

Sturm, R. (2013). Theoretical deposition of carcinogenic particle aggregates in the upper respiratory tract. *Ann. Transl. Med*. **1**, 25.

Tamura, T., Hou, J., Goldenberg, R. L., Johnston, K. E., and Cliver, S. P. (1999). Gender difference in cord serum ferritin concentrations. *Biol. Neonate* **75**, 343–349.

Terzano, C., Di Stefano, F., Conti, V., Graziani, E., and Petroianni, A. (2010). Air pollution ultrafine particles: Toxicity beyond the lung. *Eur. Rev. Med. Pharmacol. Sci*. **14**, 809–821.

Todorich, B., Pasquini, J. M., Garcia, C. I., Paez, P. M., and Connor, J. R. (2009). Oligodendrocytes and myelination: The role of iron. *Glia* **57**, 467–478.

Volpe, J. J. (2003). Cerebral white matter injury of the premature infant-more common than you think. *Pediatrics* **112(1 Pt 1)**, 176–180.

Wang, X., Rousset, C. I., Hagberg, H., and Mallard, C. (2006). Lipopolysaccharide-induced inflammation and perinatal brain injury. *Semin. Fetal Neonatal Med*. **11**, 343–353.

Willmore, L. J., and Triggs, W. J. (1991). Iron-induced lipid peroxidation and brain injury responses. *Int. J. Dev. Neurosci*. **9**, 175–180.

Yackerson, N. S., Zilberman, A., Todder, D., and Kaplan, Z. (2013). The influence of air-suspended particulate concentration on the incidence of suicide attempts and exacerbation of schizophrenia. *Int. J. Biometeorol*. **58(1)**, 61–67.

Zacharski, L. R., Ornstein, D. L., Woloshin, S., and Schwartz, L. M. (2000). Association of age, sex, and race with body iron stores in adults: Analysis of nhanes iii data. *Am. Heart J*. **140**, 98–104.

Zatta, P., Raso, M., Zambenedetti, P., Wittkowski, W., Messori, L., Piccioli, F., Mauri, P. L., and Beltramini, M. (2005). Copper and zinc dismetabolism in the mouse brain upon chronic cuprizone treatment. *Cellular and Molecular Life Sciences: CMLS* **62**, 1502–1513.

Zhang, X., Surguladze, N., Slagle-Webb, B., Cozzi, A., and Connor, J. R. (2006). Cellular iron status influences the functional relationship between microglia and oligodendrocytes. *Glia* **54**, 795–804.